hdr-CIELAB and hdr-IPT: Simple Models for Describing the Color of High-Dynamic-Range and Wide-Color-Gamut Images

Mark D. Fairchild and David R. Wyble, Rochester Institute of Technology, Munsell Color Science Laboratory, Rochester, NY/USA

Abstract

*The CIE 1976 L*a*b* Color Space, CIELAB, has been widely and successfully used in a variety of applications including digital color imaging, color image quality, and color management. One of its shortcomings, lack of hue linearity, is a critical problem in color gamut mapping and has been addressed by the IPT color space which is widely used in this domain. One limitation with both of these spaces is their applicability to color problems in high-dynamic-range (HDR) imaging. This is caused by their hard intercepts at zero luminance/lightness and by their uncertain applicability for colors brighter than diffuse white. To address these HDR questions, two newly formulated color spaces are proposed for further testing and refinement, hdr-CIELAB and hdr-IPT. They are simply based on replacing the power-function nonlinearities in CIELAB and IPT with a more physiologically plausible hyperbolic function, known as the Michaelis-Menten equation, optimized to most closely simulate the original color space for the diffuse reflecting color domain. The formulation of these proposed models is described along with some preliminary evaluations using Munsell data in comparison with CIELAB, IPT, and CIECAM02.*

Introduction

The development, implementation, and testing of color imaging systems is intimately tied to the color science tools available, namely the colorimetric and color appearance spaces that are adopted for use.[1] W. David Wright, one of the fathers of colorimetry, is famously quoted as saying that the development of color television was so closely tied to the CIE system of colorimetry that if it hadn't already existed, it would have had to be invented to allow for the invention of color TV.[2] However, sometimes, color spaces can limit the performance of color imaging systems such as when nonlinear lines of constant perceived hue produce unacceptable results in color gamut mapping,[3] or poor chromatic adaptation models preclude the transformation of color image information from one medium to another,[4] or when observer metamerism creates discrepancies between colorimetric predictions and observed colors.[5]

Another such difficulty arises when working with high-dynamic-range imaging systems. This is the fact that color spaces such as CIELAB were inherently derived for applications with reflecting colored objects under a single uniform illumination.[6] This, by definition is a low-dynamic-range environment limited to reflectances ranging from glossy black to diffuse white. The CIELAB space was not derived for, and has not been tested for, HDR stimuli that range in luminance/lightness from many orders of magnitude below diffuse white to many orders-of-magnitude above diffuse white. This limitation has been troublesome in, for example, the colorimetric calibration and characterization of HDR display systems.[7] How does one meaningfully describe the color difference of two stimuli with luminance levels relative to diffuse white of 0.0001 or 10,000?

Similarly, the IPT color space was derived to solve one of these problems. IPT was formulated to predict constant hue angle for stimuli of constant perceived hue significantly better than CIELAB.[8.9] This is very useful for gamut mapping algorithms that aim to preserve perceived hue while increasing or decreasing perceived chroma or lightness to remove violations of gamut boundaries.[10]

Useful and reliable color spaces will become more important in the development, implementation, and commercialization of HDR imaging systems (capture, processing, and display) in the coming years. Recent developments have shown the near-term viability of capture systems,[11] processing architectures,[12] and displays.[13] Commercial systems in all three domains are becoming readily available.

This paper proposes two modified color spaces, hdr-CIELAB and hdr-IPT, to begin to address some of the problems of HDR colorimetry. They are not intended as final solutions, but rather proposals that address HDR problems and provide starting points for further collection of visual data, refinement, testing and application. The basic structure of these spaces is to replace power-function-based compressive nonlinearities with sigmoidal functions (having a threshold toe and saturating shoulder like the characteristic tone reproduction curves of imaging systems) that are both more physiologically plausible and well-behaved at extreme high and low relative luminance levels. The well-known Michaelis-Menten equations are adopted and optimized for this purpose.[14] Such application of this functional form has already been successfully demonstrated in a modified form of the CIECAM02 color appearance model.[15,16] The initial derivation of hdr-CIELAB and hdr-IPT is given in the following sections along with some testing using Munsell colors and some preliminary data on lightness scaling above diffuse white.

Derivation and Formulation of hdr-CIELAB

The derivation of hdr-CIELAB is very straightforward. The CIELAB L* equation was replaced with a Michaelis-Menton equation with the following constraints. The semi-saturation constant was set to 0.184, which represents the relative luminance of a stimulus with and L* of 50. That becomes the one point where the two systems match perfectly and also makes physiological sense of putting the assumed mid-gray background as the point where stimulus contrast changes from decremental to incremental.

Second an offset of 0.02 was specified under the assumption that about 2% of diffuse white represents a reasonable level of visual noise for complex stimuli. This leaves only the exponent in the Michealis-Menten equation to be optimized. It was optimized to minimize the difference between the Michealis-Menten formulation and CIELAB L* for the L* range from 0 to 100 in relative luminance steps of 0.01. The resulting exponent was 1.50. The sum of errors in L* for the fit was -3.9 and the RMS error was 5.8. Figure 1 illustrates the L* function and fitted Michealis-Menten function, Eq. 1, as a function of relative luminance from 0 to 1.5.

$$f(\omega) = 100\frac{\omega^{\varepsilon}}{\omega^{\varepsilon} + 0.184^{\varepsilon}} + 0.02 \quad (1)$$

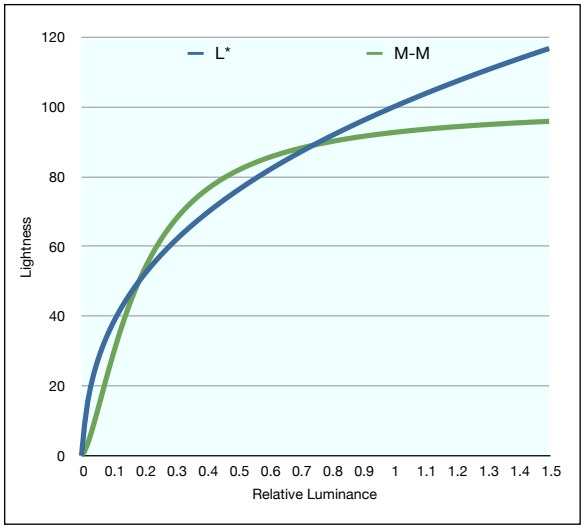

Figure 1. CIELAB L and fitted Michaelis-Menten functions of relative luminance in the range from 0-1.5.*

For imaging applications it is sometimes necessary to adjust the compressive nonlinearity to account for changes in surround relative luminance (Bartleson-Breneman) or absolute luminance level (Stevens Effect).[1] This is accomplished by modifying the exponent in the Michealis-Menten function, ε, using factors to account for surround, *sf*, and luminance level, *lf*, as shown in Eqs. 3-5. Y_s is the relative luminance of the surround and Y_{abs} is the absolute luminance of the scene diffuse white in cd/m^2.

$$\varepsilon = 1.50 \cdot sf \cdot lf \quad (2)$$

$$sf = 1.25 - 0.25(Y_s/0.184) \qquad (0 \le Y_s \le 1.0) \quad (3)$$

$$lf = \log(318)/\log(Y_{abs}) \quad (4)$$

The formulation of the full hdr-CIELAB space is then given by Eqs. 5-9 by simply replacing the CIELAB cube-root-based function with Eq. 1 and adjusting the normalization of the chroma dimensions by a factor of 1/100 to account for the scaling to 100 in Eq. 1.

$$L_{hdr} = f(Y/Y_n) \quad (5)$$

$$a_{hdr} = 5\left[f(X/X_n) - f(Y/Y_n)\right] \quad (6)$$

$$b_{hdr} = 2\left[f(Y/Y_n) - f(Z/Z_n)\right] \quad (7)$$

$$C_{hdr} = \sqrt{a_{hdr}^2 + b_{hdr}^2} \quad (8)$$

$$h_{hdr} = \tan^{-1}(b_{hdr}/a_{hdr}) \quad (9)$$

Derivation and Formulation of hdr-IPT

The derivation of hdr-IPT followed the same procedure. The IPT exponential nonlinearity (power function with exponent 0.43) was replaced with a Michaelis-Menton equation with the same constraints. The exponent in the Michealis-Menten equation was optimized to minimize the difference between the Michealis-Menten formulation and IPT I dimension for the I range from 0 to 1 in relative luminance steps of 0.01. The resulting exponent was 1.38. The sum of errors in I for the fit was -0.011 and the RMS error was 0.061. Figure 2 illustrates the I function and fitted Michealis-Menten function, Eq. 10, as a function of relative luminance from 0 to 1.5.

$$f(\omega) = 100\frac{\omega^{\varepsilon}}{\omega^{\varepsilon} + 0.184^{\varepsilon}} + 0.02 \quad (10)$$

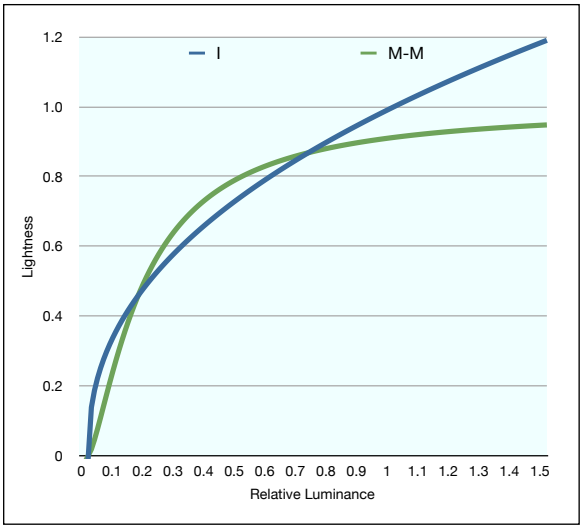

Figure 2. IPT I and fitted Michaelis-Menten functions of relative luminance in the range from 0-1.5.

The exponent in the Michealis-Menten function, ε, is again modified using factors to account for surround, *sf*, and luminance level, *lf*, as shown in Eqs. 11-13.

$$\varepsilon = 1.38 \cdot sf \cdot lf \quad (11)$$

$$sf = 1.25 - 0.25(Y_s/0.184) \qquad (0 \le Y_s \le 1.0) \quad (12)$$

$$lf = \log(318)/\log(Y_{abs}) \tag{13}$$

The formulation of the full hdr-IPT space is then given by Eqs. 14-20 by simply replacing the IPT 0.43 power function with Eq. 9.

$$\begin{bmatrix} L \\ M \\ S \end{bmatrix} = \begin{bmatrix} 0.4002 & 0.7075 & -0.0807 \\ -0.2280 & 1.1500 & 0.0612 \\ 0.0 & 0.0 & 0.9184 \end{bmatrix} \begin{bmatrix} X_{D65} \\ Y_{D65} \\ Z_{D65} \end{bmatrix} \tag{14}$$

$$\begin{aligned} L' &= f(L); & L \geq 0 \\ L' &= -f(-L); & L < 0 \end{aligned} \tag{15}$$

$$\begin{aligned} M' &= f(M); & M \geq 0 \\ M' &= -f(-M); & M < 0 \end{aligned} \tag{16}$$

$$\begin{aligned} S' &= f(S); & S \geq 0 \\ S' &= -f(-S); & S < 0 \end{aligned} \tag{17}$$

$$\begin{bmatrix} I_{hdr} \\ P_{hdr} \\ T_{hdr} \end{bmatrix} = \begin{bmatrix} 0.4000 & 0.4000 & 0.2000 \\ 4.4550 & -4.8510 & 0.3960 \\ 0.8056 & 0.3572 & -1.1628 \end{bmatrix} \begin{bmatrix} L' \\ M' \\ S' \end{bmatrix} \tag{18}$$

$$C_{hdr-IPT} = \sqrt{P_{hdr}^2 + T_{hdr}^2} \tag{19}$$

$$h_{hdr-IPT} = \tan^{-1}\left(T_{hdr}/P_{hdr}\right) \tag{20}$$

Appearance Predictions of Munsell Colors

Wyble and Fairchild[17] published an analysis of various color appearance models using the Munsell Renotation data[18] in 2000. That analysis included the CIELAB, IPT and CIECAM97s models and used only those samples found in the gamut of the 1929 *Munsell Book of Color*. In the current analysis, similar computations were completed and visualized below. However, this analysis used the full set of real Munsell data points to provide a wider color gamut and included CIECAM02 and the two new spaces derived in this paper in addition to CIELAB and IPT.

Lightness

Figure 3 shows the lightness predictors of the five models as a function of Munsell Value. Perfect prediction of Munsell Value would be represented by a straight line with unity slope as seen for the CIELAB model and very closely for the IPT model. CIECAM02 shows a slight nonlinearity of prediction and the two new HDR spaces exhibit their sigmoidal lightness scale behavior. This allows them to extend for a much wider range of relative luminance and provide a form that is consistent with the crispening effect[19] that was deliberately left out of the Munsell Renotation. [18]

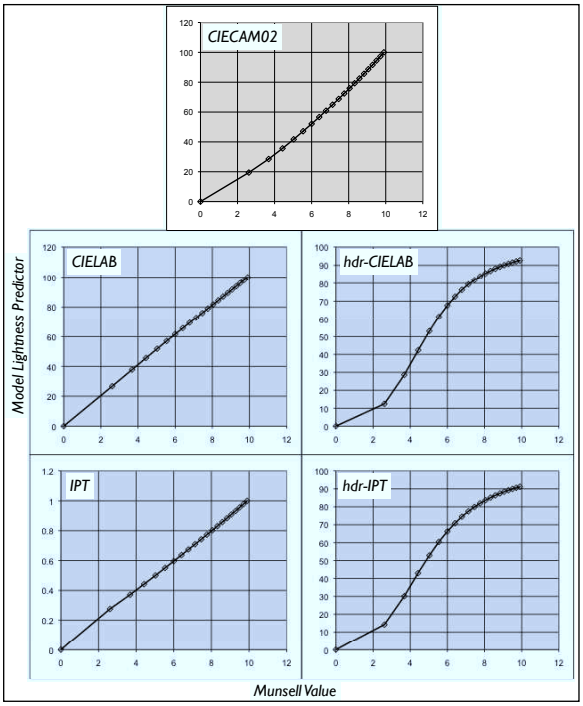

Figure 3. Model lightness predictors as a function of Munsell Value.

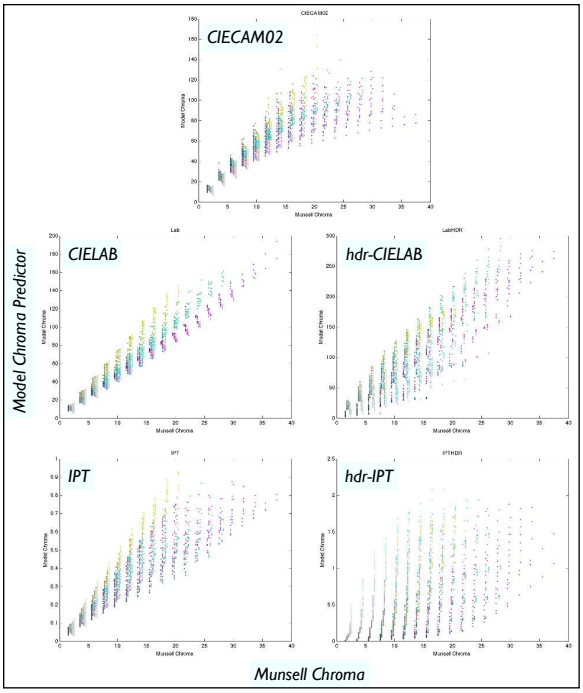

Figure 4. Model chroma predictors as a function of Munsell Chroma.

Chroma

Figure 4 shows the chroma predictors of the five models as a function of Munsell Chroma. Data points are color coded to their Munsell designations. Perfect prediction of Munsell Chroma would be represented by a straight line with unity slope and no scatter. One can see the well known compression of yellow chroma in CIELAB in comparison with the blue hues. However, it is also

clear that the CIELAB space most consistently predicts the Munsell Chroma data. IPT also has fairly linear predictions, but the spread from hue to hue is more significant. CIECAM02 also has similarly large spread on top of some nonlinear behavior. The two hdr spaces show very large spread in the chroma predictions that will require further explanation and potential refinement of the models. It is likely that some flexibility in the semi-saturation constant (and therefore the scale range of the nonlinearities) will be required to create hdr spaces that more closely approximate the original CIELAB and IPT spaces.

Hue Linearity

Fig. 5 shows the five model hue predictors as a function of Munsell Hue, again color coded by Munsell designation. Ideal results would be a perfect straight line. The well-known kink in the blue region of CIELAB is evident along with the relatively good behavior of IPT. The HDR versions of CIELAB and IPT show similar behavior with respect to hue linearity.

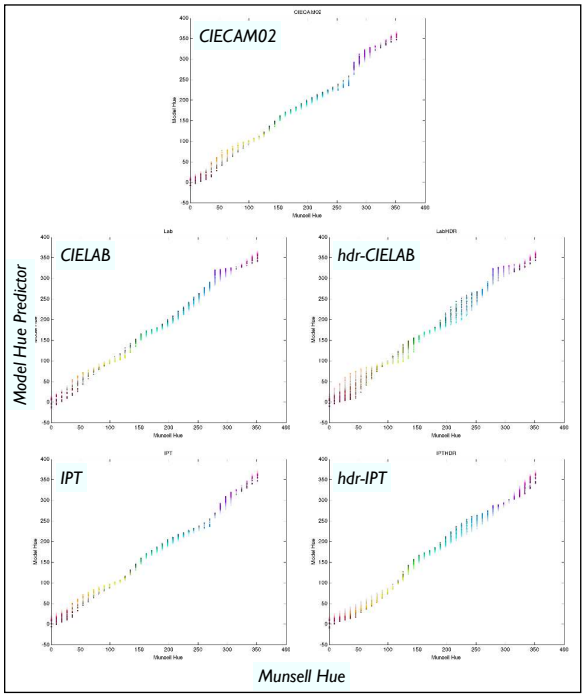

Figure 5. Model hue predictors as a function of Munsell Hue.

An alternative analysis of hue linearity is visualized in Fig. 6. In this case principal components analysis was performed on each hue slice (projected to the two chromatic dimensions) to determine the percent of variation explained by a single characteristic vector. A value of 100% would imply perfect hue linearity. Figure 6 encodes the percent of variation that is not described by the first characteristic vector (*i.e.*, the amount of variation requiring a second dimension, or curve, to describe). Each model is represented by a row in the figure with the various hues represented by columns. Dark areas represent poor hue linearity with values represented by black meaning greater than about 10% variance is not described by one dimension. Mid-gray areas represent about 3% residual variation and white areas represent nearly perfect hue linearity. The rightmost column represents the average values. It can be seen that IPT shows its characteristic good hue linearity and hdr-IPT is similar and almost identical on average. CIECAM02 and CIELAB illustrate similar performance slightly worse than IPT and hdr-CIELAB introduces some significant hue nonlinearities due to the sigmoidal nonlinearities that might need attention in a future revision.

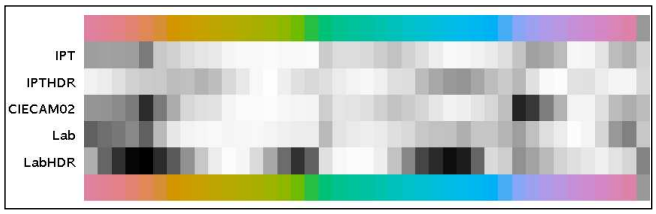

Figure 6. Visualization of PCA analysis on the dimensionality of constant hue lines. Dark entries indicate that a significant amount of variation requires two dimensions to describe (an indication of hue nonlinearity).

Hue Spacing

Hue spacing was evaluated by examining the hue angle distance between each neighboring Munsell Hue in each color space. Since there are 40 hue samples in the Munsell Renotation, each should be separated by 9 degrees in hue angle for uniform hue spacing. (Note it is possible to have good spacing with poor linearity and vice versa.) T-tests were performed to test the hypothesis that the average distance between adjacent hue planes is 9 degrees. A $p>0.05$ indicates that they hypothesis cannot be rejected. The visualization in Fig. 7 renders the p values for each hue and the average in the last column. P values of near zero are shown as black and indicate poor hue spacing. P values rendered in white are near 1.0 with the mid gray representing $p = 0.5$. Each space shows significant deviation from equal hue spacing with IPT slightly worse than the others on average.

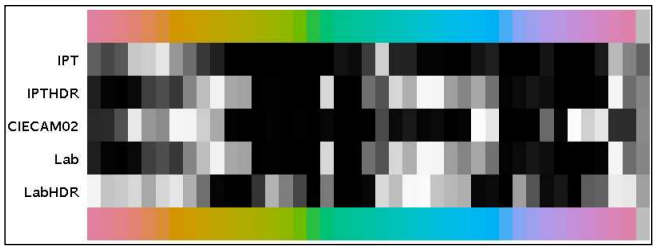

Figure 7. Results of t-tests on hue spacing. If each Munsell hue was equally spaced from its neighbors for a given model, the row of squares would be white. Black areas indicates hues with poor spacing.

Wide-Range Lightness Predictions

Recently experiments have been completed to scale perceived lightness and lightness differences for a range of neutral stimuli with lightnesses well above that of diffuse white (*i.e.*, with L*>100)[20]. These preliminary data were graciously made available by to evaluate the hdr-CIELAB and hdr-IPT lightness scales in this extended range. The results are shown in Fig. 8 on log-log axes. CIELAB L* and IPT I predict the data well for lightness greater than diffuse white while hdr-CIELAB L_{hdr} and hdr-IPT I_{hdr} predict the data better for lightness less than diffuse white (all models were normalized to predict a lightness of 100 for a relative luminance of 1.0. Since this is just one experiment on

scaling wide-range lightness, it is premature to adjust either model to specifically fit these data. However the discrepancies well illustrate that the models might require some fine tuning of their exponents or semi-saturation constants. Alternatively it might be the case that adaptation in wide-range lightness scaling needs to be better understood.

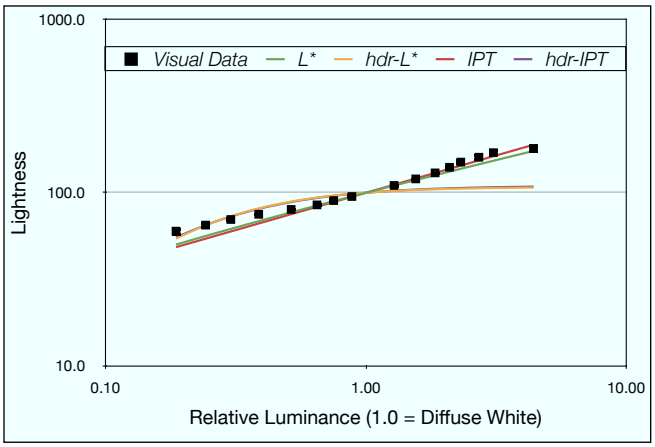

Figure 8. Prediction of lightness scaling data in the range from L = 60 to L* = 180. Symbols are visual data and lines are model predictions. 95% confidence intervals on the experimental data are approximately the same size as the plotting symbols and thus obscured by the symbols themselves.*

Conclusions

Two new color spaces were proposed, hdr-CIELAB and hdr-IPT, to allow extension of the CIELAB and IPT color spaces for use in HDR imaging applications. Their overall performance in predicting Munsell Renotation appearances is similar to the traditional versions of these spaces. However some discrepancies, especially in chroma predictions, do show up that warrant further investigation. These spaces provide interesting combinations of colorimetric fidelity and physiological plausibility and pose interesting new questions for developers of color spaces and imaging systems. At this point, these spaces should be considered proposals as there is certainly a need for more testing, collection of more HDR visual data, and refinement of the models. They do, however, show great promise for future applications in color specification, device characterization, image difference metrics and image quality evaluation.

Acknowledgements

This research was supported by the RIT Munsell Color Science Laboratory.

References

1. M.D. Fairchild, *Color Appearance Models, Second Edition*, Wiley-IS&T Series in Imaging Science and Technology, Chichester, UK (2005).
2. W.D. Wright, 50 years of the 1931 CIE standard observer for colorimetry, *AIC Color 81*, Paper A3 (1981).
3. G.J. Braun, F. Ebner, and M.D. Fairchild, Color gamut mapping in a hue-linearized CIELAB color space, *IS&T/SID 6th Color Imaging Conference*, Scottsdale, 163-168 (1998).
4. M.D. Fairchild, Chromatic adaptation to image displays, *TAGA* **2**, 803-824 (1992).
5. M.D. Fairchild and D.R Wyble, Mean observer metamerism and the selection of display primaries, *IS&T/SID 15th Color Imaging Conference*, Albuquerque, 151-156 (2007).
6. A.R. Robertson, The CIE 1976 color-difference formulae, *Color Res. Appl.* **2**, 7-11 (1977).
7. J.A. Ferwerda and S. Luka, A high resolution high dynamic range display for vision research, *Journal of Vision* **9**, 346 (2009).
8. F. Ebner, and M.D. Fairchild, Development and testing of a color space (IPT) with improved hue uniformity, *IS&T/SID 6th Color Imaging Conference*, Scottsdale, 8-13 (1998).
9. M.D. Fairchild and G.M. Johnson, The iCAM framework for image appearance, differences, and quality, *J. Elec. Imaging* **13**, 126-138 (2004).
10. R.L. Heckaman and M.D. Fairchild, Brighter, more colorful colors and darker, deeper colors based on a theme of brilliance, *Color Research and Application* **33**, in press (2010).
11. M.D. Fairchild, The HDR photographic survey, *IS&T/SID 15th Color Imaging Conference*, Albuquerque, 233-238 (2007).
12. E. Reinhard, G. Ward, P. Debevec, and S. Pattanaik, *High Dynamic Range Imaging: Acquisition, Display, and Image Based Lighting*, Morgan Kaufmann, San Francisco (2005).
13. H. Seetzen, W. Heidrich, W. Stuerzlinger, G. Ward, L. Whitehead, M. Trentacoste, A. Ghosh, A. Vorozcovs, High-dynamic-range display systems, *Proceedings of SIGGRAPH '04*, 760-768 (2004).
14. K.I. Naka and W.A.H. Rushton, S-potentials from colour units in the retina of fish (Cyprinidae), *J. Physiology* **185**, 536–555 (1966).
15. A.O. Akyüz and E. Reinhard, Color appearance in high-dynamic-range imaging, *J. Electronic Imaging* **15**, 033001 (2006).
16. Timo Kunkel and Erik Reinhard, A neurophysiology-inspired steady-state color appearance model, *Journal of the Optical Society of America A* **26**, 776-782 (2009).
17. D.R. Wyble and M.D. Fairchild, Prediction of Munsell appearance scales using various color appearance models, *Color Research and Application* **25**, 132-144 (2000).
18. S.M. Newhall, Preliminary report of the O.S.A. subcommittee on the spacing of the Munsell colors, *J. Opt. Soc. Am.* **30**, 617-645 (1940).
19. C.C. Semmelroth, Prediction of lightness and brightness on different backgrounds, *J. Opt. Soc. Am.* **60**, 1685-1689 (1970).
20. P.-H. Chen, M.D. Fairchild, and R.S. Berns, Scaling lightness perception and differences above and below diffuse white, *IS&T/SID 18th Color Imaging Conference*, San Antonio, *in press* (2010).

Author Biography

Mark D.Fairchild is Associate Dean for Research and Graduate Education of the College of Science at Rochester Institute of Technology. He is also Professor of Color and Imaging Science and Coordinator RIT's M.S. and Ph.D. programs in Color Science. He is a Fellow of IS&T and was recently presented with the society's Raymond C. Bowman award for mentoring future researchers in the field.

David R. Wyble is a Color Scientist specializing in color measurement system research in the RIT Munsell Color Science Laboratory. He has a Ph.D. in Imaging Systems from Chiba University.